Interannual variability of the frontal activity in the Southern Hemisphere: relationship with atmospheric circulation and precipitation over southern South America

Josefina Blázquez & Silvina A. Solman

ONLINE
FIRST

Springer

Springer

CrossMark

Interannual variability of the frontal activity in the Southern Hemisphere: relationship with atmospheric circulation and precipitation over southern South America

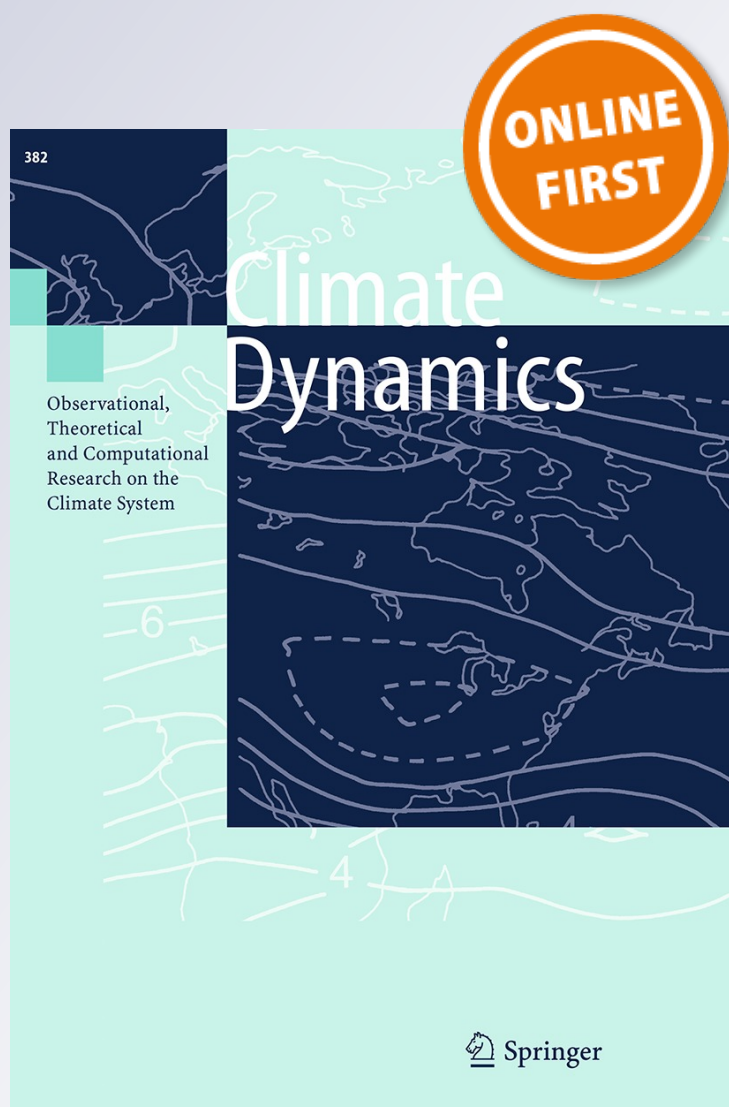**Josefina Blázquez[1] · Silvina A. Solman[1]**

Abstract The interannual variability of the frontal activity over the western Southern Hemisphere and its linkage with the variability of the atmospheric circulation and precipitation over southern South America is studied. The analysis is focused on the austral winter and spring seasons. The frontal activity is represented by an index defined as the product between the horizontal gradient of temperature and the relative vorticity at 850 hPa (FI) and is computed from the ERA Interim and NCEP2 reanalysis. For the two seasons the main mode of variability of FI, as depicted by the first Empirical Orthogonal Function, presents centres of action located in the southern part of the western Southern Hemisphere. This pattern is present in the two reanalysis datasets. The correlation coefficients between the principal component of the leading mode of FI and the two main modes of the 500 hPa geopotential height indicate that both the ENSO-mode and the SAM modulate the leading pattern of FI in winter while during the spring season the ENSO-mode controls the FI variability. The variability of the FI has a robust influence on the interannual variability of precipitation over southern South America and adjacent oceans. Over the continent, it was found that the pattern of precipitation anomalies associated with the variability of the FI depicts significant signals over southeastern South America (SESA), centre and south of Chile for winter and over SESA and southeastern Brazil for spring and agrees with the pattern of the leading mode of precipitation variability over southern South America.

1 Introduction

The main modes of variability of the Southern Hemisphere (SH) atmospheric circulation at the interannual timescales have been widely documented in the literature (Kidson 1988, 1999; Kiladis and Mo 1998; Mo 2000; Trenberth et al. 2005; among others). The leading mode is the Southern Annular Mode (SAM), which consists in a height anomaly pattern of wave one over Antarctica and height anomalies of opposite sign at midlatitudes. When the SAM is in its positive phase (negative anomalies over the polar latitudes and positive anomalies over the midlatitudes; Thompson and Wallace 2000) the westerlies intensify towards polar latitudes. The second and third modes of variability are related with the El Niño-Southern Oscillation (ENSO) phenomenon (hereinafter ENSO-modes). These modes are characterized a wave pattern emanating from the equatorial Pacific associated with anomalous heating and propagating towards the southeast, reaching South America (SA).

It is widely known that the interannual variability of these atmospheric circulation patterns affects the precipitation anomalies over SA. Mo and Nogés Paegle (2001) have shown that the first ENSO-mode (in its positive phase: El Niño event) impacts on the winter precipitation over SA generating negative anomalies over Peru and Brazil and positive

✉ Josefina Blázquez
blazquez@cima.fcen.uba.ar

Silvina A. Solman
solman@cima.fcen.uba.ar

[1] Centro de Investigaciones del Mar y la Atmósfera (CIMA-CONICET/FCEN-UBA), Departamento de Ciencias de la Atmósfera y los Océanos (FCEN-UBA), Instituto Franco Argentino del Clima y sus Impactos (UMI IFAECI/CNRS), Ciudad Universitaria Pabellón II Piso 2, C1428EGA Buenos Aires, Argentina

Springer

anomalies further to the south. Silvestri and Vera (2003) studied the impact of SAM on precipitation over SESA and found that during the spring the positive phase of the SAM is associated with negative precipitation anomalies. Moreover, Grimm (2011) identified the modes of variability of precipitation over South America associated to ENSO variability for all seasons: in winter the first mode shows the main signal located over SESA, while in spring a dipole pattern between SESA and central-east Brazil is evident.

On the other hand, the variability of the atmospheric circulation has an influence in the synoptic systems that affect mainly subtropical and high latitudes of the SH. Vera (2003) studied the interannual and interdecadal variation of the storm tracks in the SH and found that the leading mode of the storm tracks exhibits a significant variability on the interannual timescales, which in turn is associated with ENSO. Rao et al. (2003) found a connection between the storm track variability in the SH and the SAM at the inter-annual timescales: during the positive phase of SAM the mid-latitude storm track is intensified. Recently, Rudeva and Simmonds (2015) explored the relationship between fronts and the main modes of variability of atmospheric circulation and found that El Niño reduces the number of fronts in the South Pacific in the band 45°S–60°S and intensifies the number of fronts at lower and higher latitudes.

It is extensively known that precipitation is largely associated with the passage of frontal systems (Bjerknes and Solberg 1922; Browning and Roberts 1994), especially during winter. For example, Catto et al. (2012) found that a large proportion of precipitation in the midlatitudes of SH is associated with fronts; furthermore they found that 90 % of the precipitation in the storm tracks regions is due to frontal systems.

The studies referred above suggest that the variability of the large-scale atmospheric circulation has a strong impact on the precipitation anomalies over the SH. In addition, several studies cited above emphasize, on one hand, that the large-scale atmospheric circulation variability has an impact on the variability of the synoptic activity and, on the other hand, precipitation is largely associated with frontal systems. In fact, recently Blázquez and Solman (2016) (hereinafter BS16) have studied how the intraseasonal variability of the large scale circulation controls the variability of the frontal activity that in turn affects the variability of precipitation in the vicinity of SA.

Therefore, taking into account the discussion above and the results of BS16 one of the objectives of this study is on one hand to explore the variability of the frontal activity at the interannual timescales and on the other hand to assess how this variability is conditioned by the variability of the atmospheric circulation. The last goal of this paper is to explore how the variability of the frontal activity affects the precipitation anomalies over SA at the mentioned timescales.

This paper is organized as follows: In Sect. 2 the data and the methodology used in this study are described. The results are presented in Sect. 3 and finally a summary and conclusions are described in Sect. 4.

2 Data and methodology

In this study data from the European Centre Medium Range Weather Forecasts (ECMWF), ERA Interim reanalysis (Simmons et al. 2007; Dee et al. 2011) with 1.5° resolution; and data from National Centers for Environmental Prediction (NCEP), NCEP2 reanalysis (Kanamitsu et al. 2002) with 2.5° resolution for the period 1979–2013 were used.

All calculations were done with the two reanalysis in order to compare different datasets and with the objective of identifying robust patterns. However, the analysis is mainly based on results from the ERA Interim reanalysis dataset since it is at higher resolution, and only few results using the NCEP2 reanalysis are shown.

To represent the frontal activity and index (FI) defined by Solman and Orlanski (2010) as the relative vorticity times the local temperature gradient at 850 hPa was used:

$$FI = |\nabla T_{850 \text{ hPa}}| \times \xi_{850 \text{ hPa}}$$

The definition of FI attempts to capture frontal systems, which are associated with a strong temperature gradient and a cyclonic vorticity centre. Therefore, only cyclonic relative vorticity values were retained, and the index was set to zero otherwise. Including the local temperature gradient avoids capturing cyclonic centres not associated with fronts.

Solman and Orlanski (2014) discussed this index in depth, comparing the infrared satellite imagery with the FI index and they found high consistency between the two variables, suggesting that the FI index is a good metric to represent fronts. The FI index was previously used in Solman and Orlanski (2010) and in Blázquez and Solman (2016) to identify the intraseasonal variability of the frontal activity and its connection with the variability of precipitation and the atmospheric circulation over South America. In addition, Solman and Orlanski (2014) used the FI index to demonstrate that change of precipitation over the last 40 years over the Southern Hemisphere was largely associated with the change in the frontal activity.

To calculate this index daily data from the two reanalysis datasets were used and then seasonal means of the index were computed. To represent the atmospheric circulation, monthly values of geopotential height at 500 hPa from the reanalysis datasets were used and then averaged seasonally. For precipitation, data comes from the Global Precipitation Climatology Project (GPCP) monthly precipitation dataset (Adler et al. 2003), with 2.5° resolution for the period 1979–2013.

This study is focused on the austral extended winter season defined from May to August (MJJA) and the austral extended spring season, from September to December (SOND). Seasonal anomalies were computed by subtracting to the raw data the mean climatology for each season.

To detect the leading modes of variability of FI in the western SH (from 70°S to 15°S and 180°W 0°) the Empirical Orthogonal Function (EOF) technique was used. The reduced domain was chosen following BS16. Rotated EOF (REOF) was also calculated for FI to explore the orthogonality problem (Hannachi et al. 2007). The leading modes found were similar to those found with the unrotated EOF technique, suggesting that these modes have a physical meaning. Therefore, in this study the unrotated modes derived from the EOF technique were used.

To evaluate the relationships among FI, geopotential height and precipitation anomalies, regressions and correlations were calculated. A Fisher test was implemented to evaluate the statistical significance of the correlation coefficients using 35 degrees of freedom and a confidence level of 95 %.
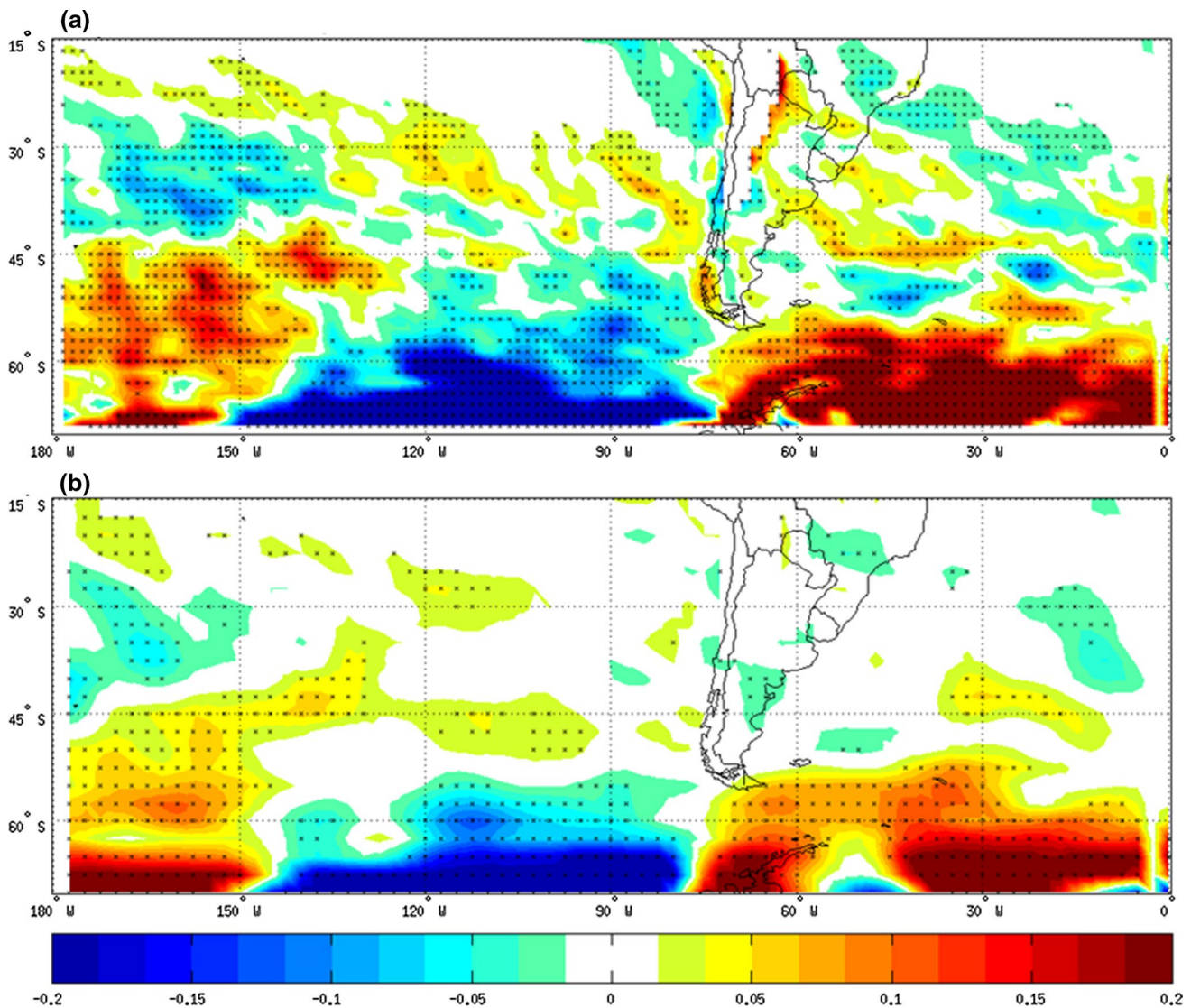
Fig. 1 Regression of the front-index anomaly field (in $1e^{-10}* °C \, m^{-1} \, s^{-1}$) against the first PC of front-index, for winter. **a** ERA Interim reanalysis, **b** NCEP2 reanalysis. *Dots* mean 95 % confidence level, according to a Fisher test

(a)

(b)
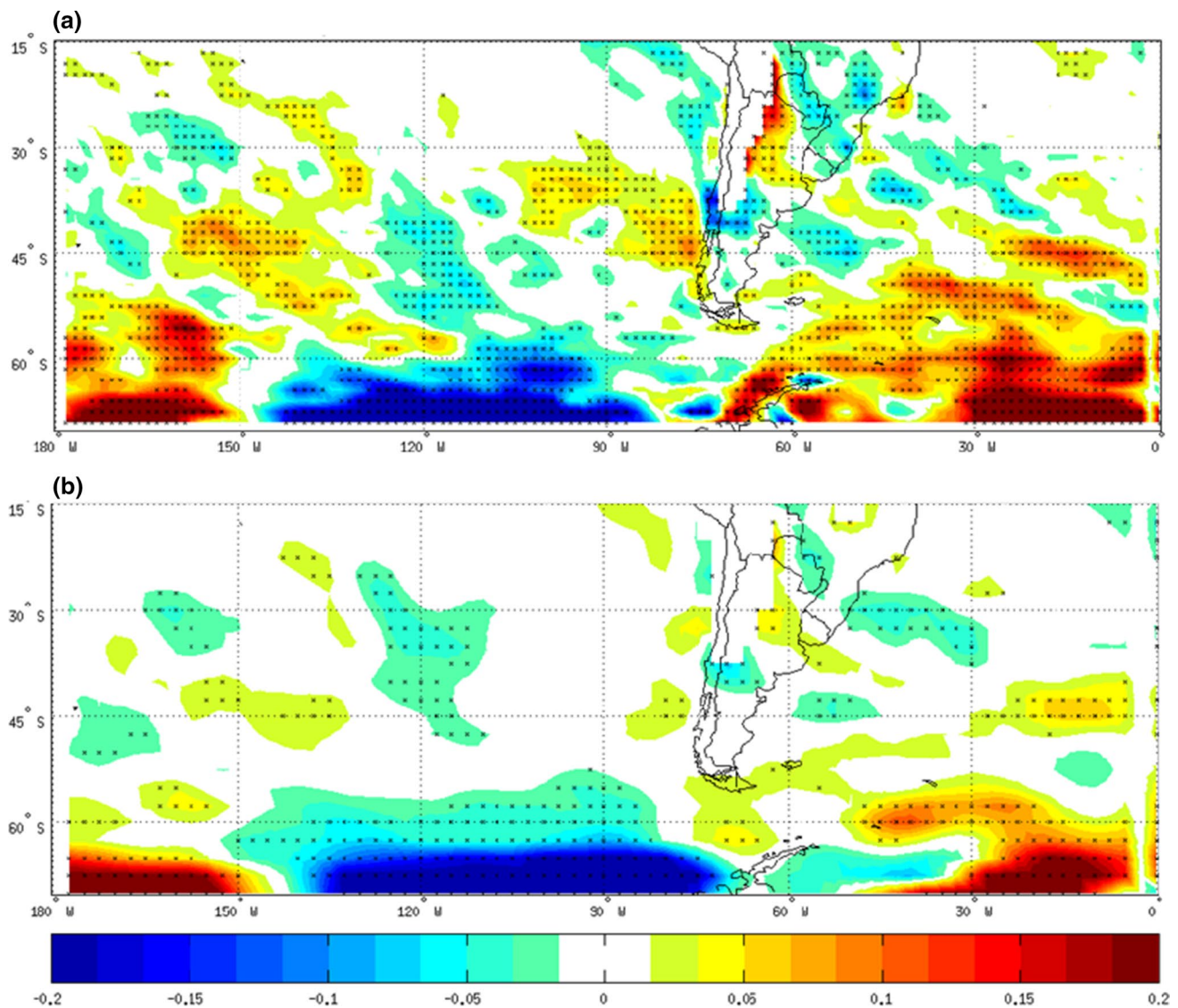
Fig. 2 Regression of the front-index anomaly field (in 1e^{-10}∗ °C m^{-1} s^{-1}) against the first PC of front-index, for spring. **a** ERA Interim reanalysis, **b** NCEP2 reanalysis. *Dots* mean 95 % confidence level, according to a Fisher test

3 Results

3.1 The main mode of variability of FI and its relationship with the variability of the atmospheric circulation

One of the main objectives of this paper is to identify the main modes of variability of the frontal activity in the SH at the interannual timescales. Figure 1 shows the spatial pattern of the first mode of variability of FI for the extended winter season (represented by the regression between the first PC of FI and the anomaly field of FI), as depicted by both ERA Interim (Fig. 1a) and NCEP2 (Fig. 1b) reanalysis datasets. The first mode explains 19 % of the total variance for the two

datasets. Comparing Fig. 1a, b, the agreement among them is apparent. The correlation coefficient between the principal component of the first mode from the ERA Interim and the NCEP2 reanalysis datasets is 0.82. This result confirms the agreement between reanalyses and suggests that these modes correspond to physical patterns. Figure 1 shows centres of positive and negative anomalies of FI located in the southern part of the domain. This pattern resembles the intraseasonal modes of FI described in BS16. The regression between the leading PC of FI and the anomalies of the 500 hPa geopotential heights (not shown) indicates that positive anomalies of FI match with negative anomalies of geopotential height and viceversa. This result suggests that the negative anomaly of FI in the southeastern Pacific Ocean is associated with a
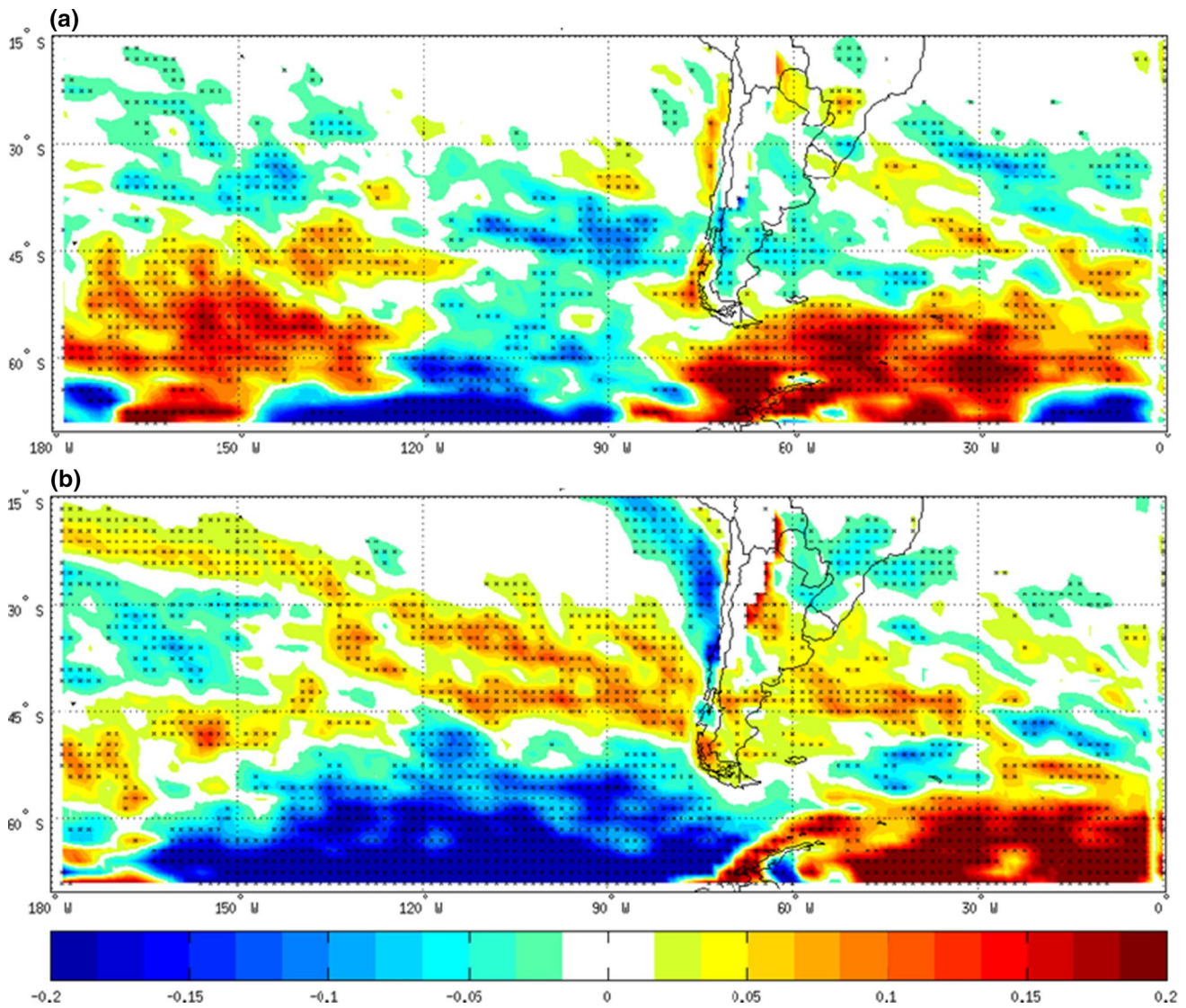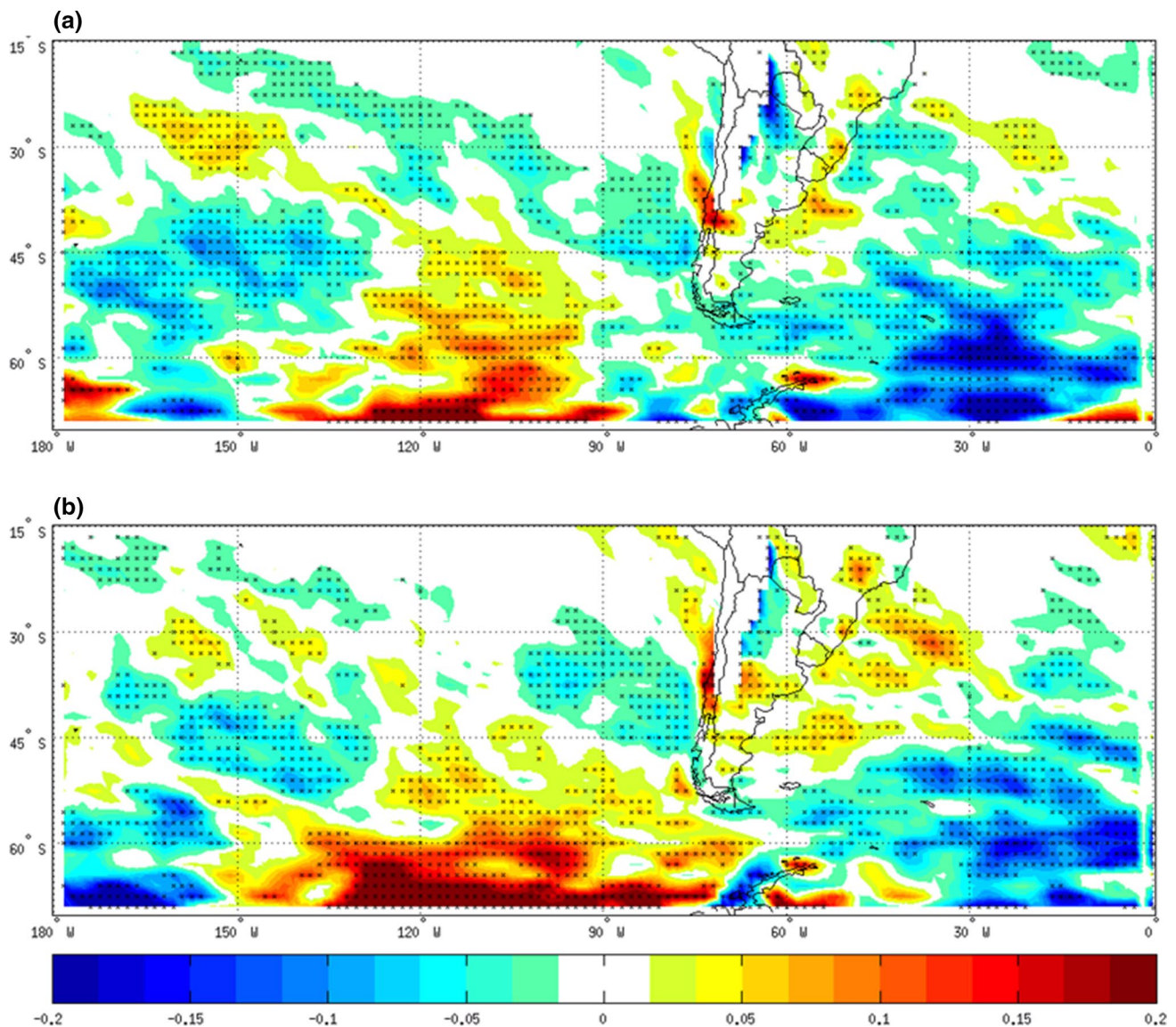
Fig. 3 Regression of the front-index anomaly field (in $1e^{-10}* \, °C \, m^{-1} \, s^{-1}$) against first (**a**) and second (**b**) PC of the 500 hPa geopotential height, for winter from the ERA Interim reanalysis dataset. *Dots* mean 95 % confidence level, according to a Fisher test

positive anomaly of geopotential height, which inhibits the evolution to the east of frontal systems.

Figure 2 shows the first leading pattern of FI for the extended spring season from both the ERA Interim and NCEP2 reanalysis datasets. The first mode displayed in Fig. 2a explains 15 % of the total variance whereas the first mode displayed in Fig. 2b explains 24 %. The correlation coefficient between PC1 of the two sets of data is 0.76. As in winter, there is a good agreement between the pattern from ERA Interim and NCEP2 reanalysis. It can be seen from Fig. 2 that the main signal is in the southern part of the domain. Compared with winter (Fig. 1), the centres of action of the first mode are located further to the south in spring. This result is expected, due to the storm tracks'

seasonal displacement, which are closely associated with frontal activity (Solman and Orlanski 2014).

The next step is to explore which are the modes of variability of the atmospheric circulation that control the modes of variability of the frontal activity. First, an EOF analysis was performed to the seasonal anomalies of the 500 hPa geopotential height for the two target seasons. The first and second modes found were the well-known SAM and ENSO modes, respectively (Kidson 1988, 1999; Kiladis and Mo 1998; Mo and Nogés Paegle 2001; Grainger et al. 2011). The regression between the first two PCs of the 500 hPa geopotential height and the FI anomalies from the ERA Interim reanalysis for winter are displayed in Fig. 3. When PC1 of 500 hPa geopotential height is positive

(a)

(b)

Fig. 4 Regression of the front-index anomaly field (in $1e^{-10}*$ °C m^{-1} s^{-1}) against first (**a**) and second (**b**) PC of the 500 hPa geopotential height, for spring from the ERA Interim reanalysis dataset. *Dots* mean 95 % confidence level, according to a Fisher test

(corresponding to the negative phase of SAM), positive anomalies of the 500 hPa heights located over the southeastern Pacific Ocean (not shown) inhibits the development of the frontal activity, with negative anomalies of FI, as depicted in Fig. 3a. In the case of the ENSO mode, positive values of PC2 of the 500 hPa geopotential height corresponds to El Niño events (not shown) with positive height anomalies at the high-latitudes of the eastern Pacific Ocean and negative height anomalies at the mid-latitudes (Garreaud and Battisti 1999). Looking at Fig. 3b it is apparent that El Niño forces the frontal systems to progress along a latitude band between 30°S and 45°S over the eastern Pacific Ocean, shifting the fronts towards a northern path. This result is in agreement with Rudeva and Simmonds

(2015) and with Solman and Menéndez (2002). Note also the resemblance between the spatial patterns displayed in Figs. 1a and 3. Moreover, the correlation coefficients between PC1 and PC2 of the 500 hPa geopotential height and PC1 of FI are 0.51 and 0.68, respectively, suggesting that at the interannual timescales, the variability of the frontal activity during the winter season is mainly conditioned by both the SAM and the ENSO modes of variability. This behaviour is also found with NCEP2 reanalysis (not shown), though with lower correlation coefficients between PCs.

Figure 4 displays the regression between PC1 and PC2 of the 500 hPa geopotential height and FI anomalies for spring, from the ERA Interim reanalysis dataset.
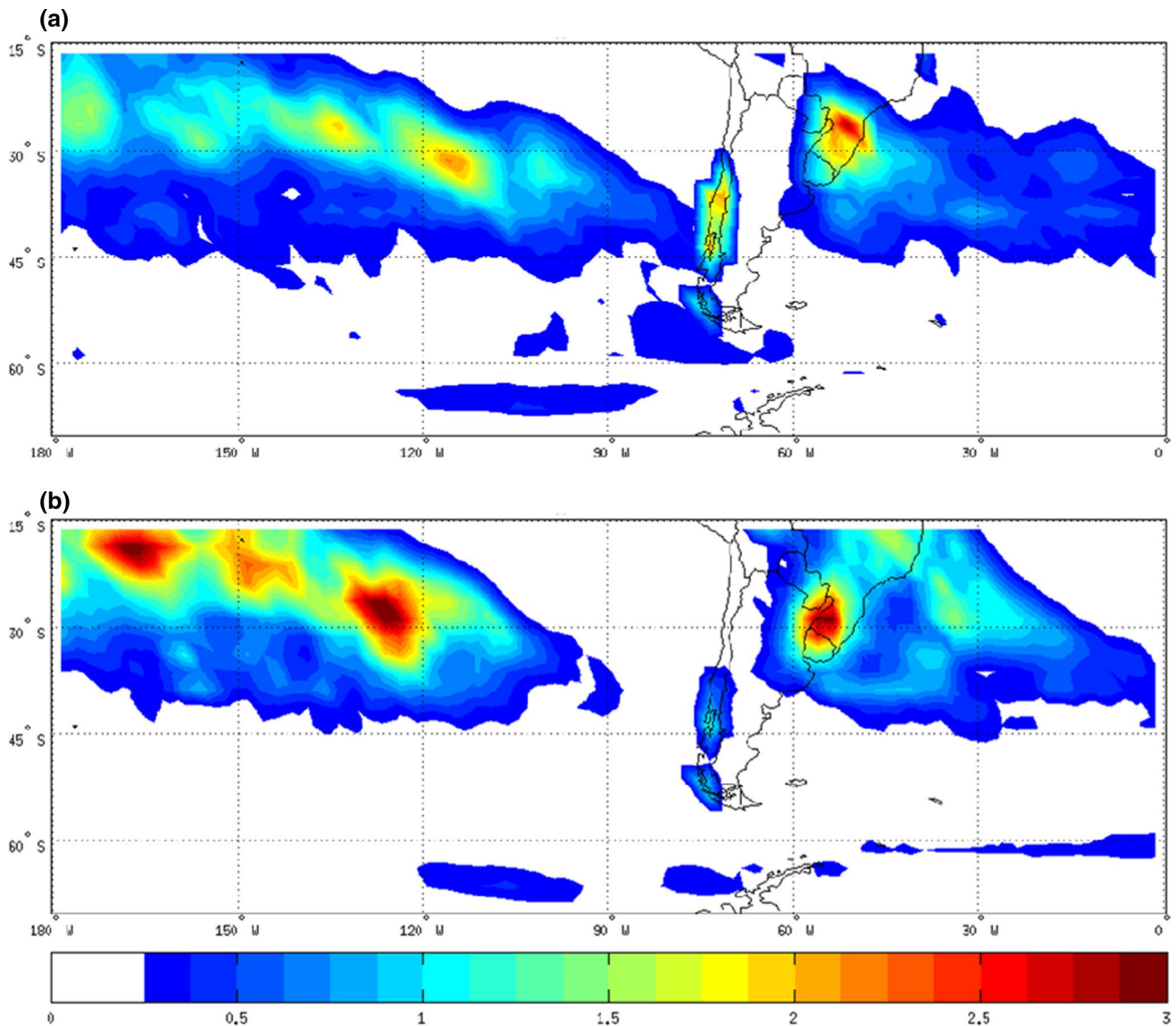
Fig. 5 Variance of seasonally precipitation from the GPCP dataset (in mm^2/day^2) for **a** winter and **b** spring. Values smaller than 0.25 mm^2/day^2 are blanked

The correlation coefficients between the two leading PCs of the 500 hPa geopotential height against the leading PC of FI are 0.34 and 0.67, respectively. This indicates that in the case of spring, the ENSO variability is the main phenomenon that controls the variability of the frontal activity. Moreover, the resemblance between Figs. 2a and 4b is remarkable. As in winter, this behaviour is also found in NCEP2 reanalysis (not shown). The positive regression over the southeastern Pacific Ocean that can be seen in Fig. 4b corresponds to negative anomalies of FI when PC2 is negative (El Niño event). This indicates that during the positive phase of ENSO the wave train that emanates from the equatorial Pacific Ocean impacts on the first mode of variability of FI decreasing (increasing) the frontal activity at high latitudes (mid-latitudes) of southeastern Pacific Ocean.

3.2 The influence of the FI variability on precipitation

Another important objective of this paper is to analyse the impact of the interannual variability of the frontal activity on the precipitation anomalies. First of all, the interannual variability of precipitation is explored for the two seasons. Such variability is shown in Fig. 5 for the western SH, computed in terms of the variance of the seasonal mean precipitation. For both winter (Fig. 5a) and spring (Fig. 5b) the largest values of variability (more than 3 mm^2/day^2) are located over the southeastern South America
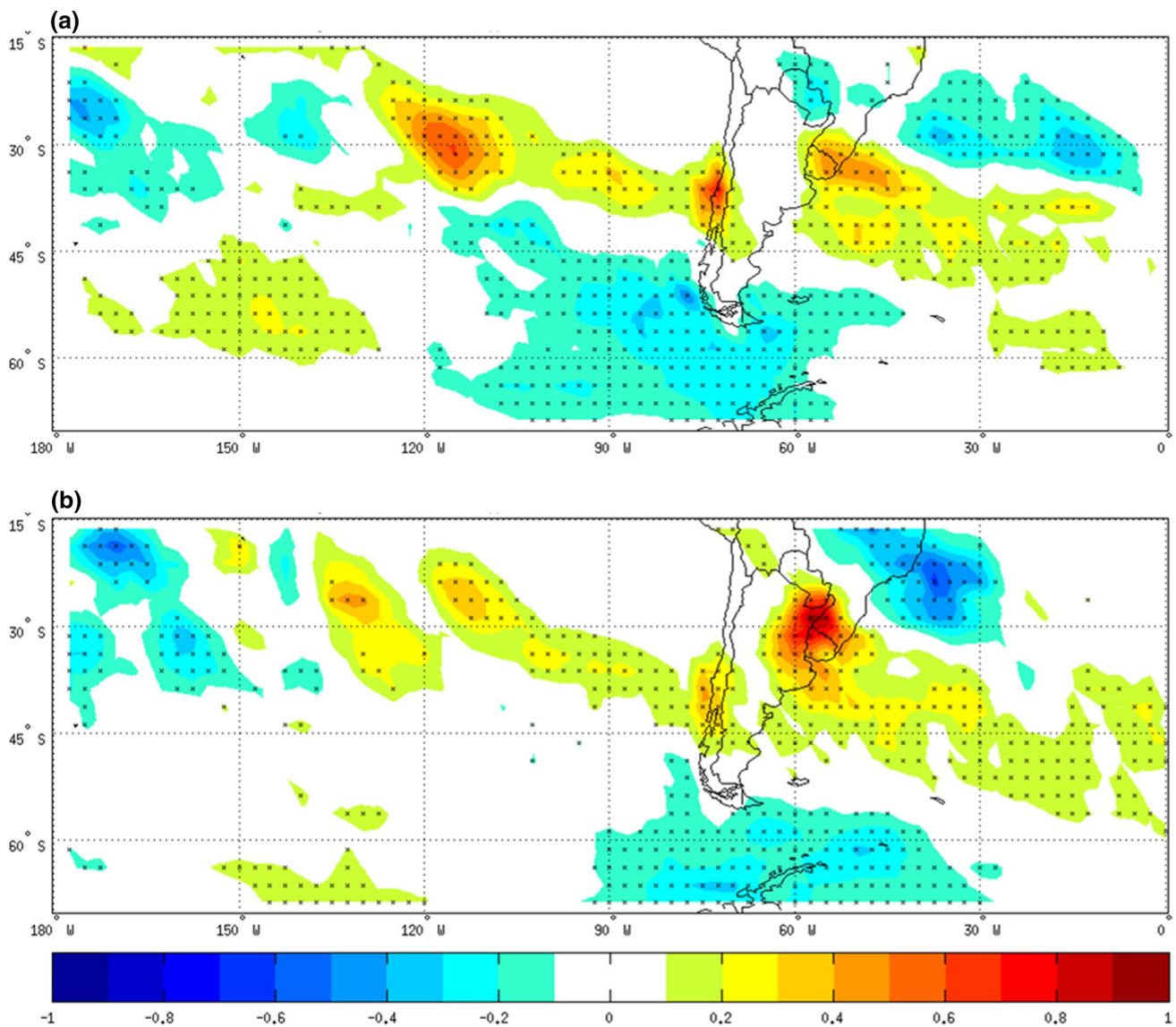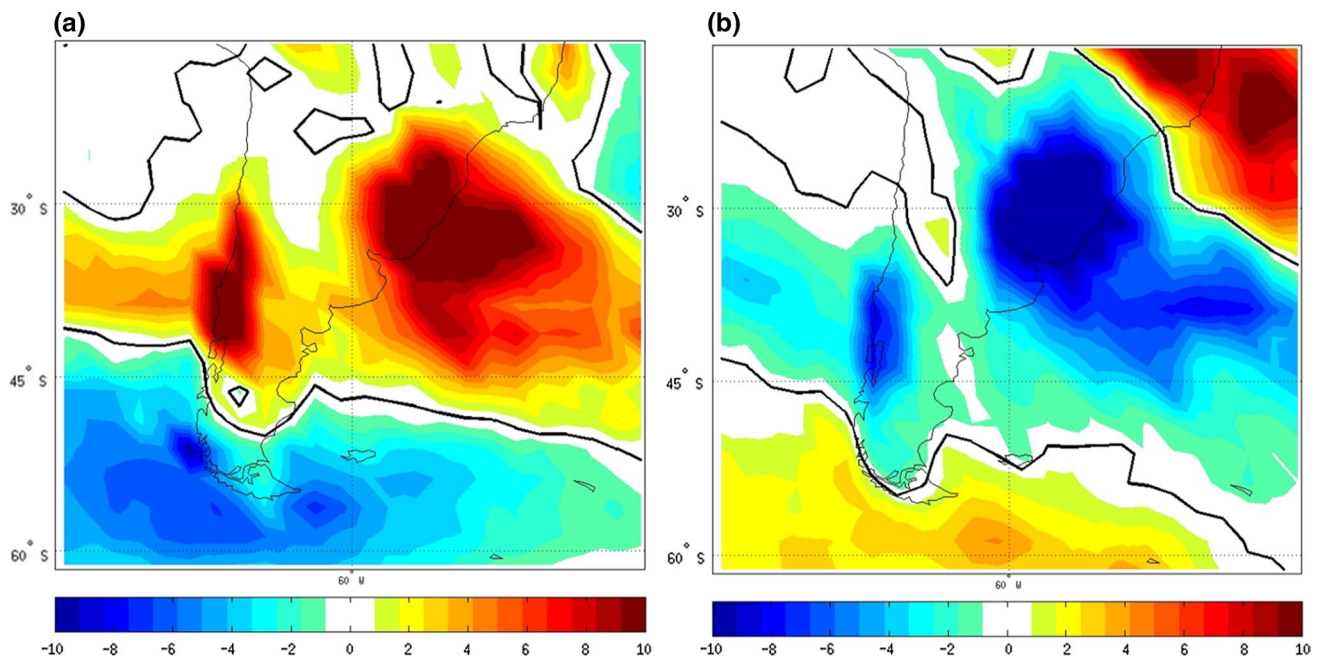
Fig. 6 Regression of the precipitation anomaly field (in mm/day) against the first PC of FI for **a** winter and **b** spring. GPCP dataset was used for precipitation and ERA Interim reanalysis for FI. *Dots* mean 95 % confidence level, according to a Fisher test. Values between ± 0.1 mm/day are blanked

(SESA) and over the mid-latitudes of the Pacific Ocean. In particular in winter the values are lower than in spring, except in the centre and south of Chile. To explore the relationship between the variability of the frontal activity and precipitation Fig. 6 displays the regression between PC1 of FI (using the ERA Interim reanalysis dataset) and precipitation anomalies from GPCP database for winter (Fig. 6a) and spring (Fig. 6b). In winter the first mode of variability of the frontal activity produces anomalies of precipitation over SESA, centre and south of Chile, over the mid-latitudes of Pacific and Atlantic Oceans and over southeastern Pacific Ocean. Positive (negative) precipitation anomalies are consistent with positive (negative) FI anomalies (see Fig. 1a) suggesting that the variability of the frontal activity controls the precipitation anomalies at the interannual timescales. In spring (Fig. 6b), the frontal activity variability causes a pattern of precipitation anomalies over and in the vicinity of the continent with positive (negative) rainfall anomalies over regions where the frontal activity is enhanced (inhibited). These results were also obtained using NCEP2 reanalysis (not shown). Note that the regions where the interannual variability of precipitation is large (Fig. 5) agree with those regions dominated by the influence of the frontal activity (Fig. 6), particularly SESA, south and centre of Chile, mid-latitudes of Pacific and Atlantic Oceans. This indicates that the main mode of

Fig. 7 The leading EOF of the precipitation anomaly field from the GPCP dataset for (unitless) **a** winter and **b** spring

variability of the frontal activity has a high impact on the precipitation variability over the western part of HS in both winter and spring.

The analysis presented above highlights that the interannual variability of the frontal activity has an impact on the precipitation anomalies. However, it is worth evaluating to what extent the interannual variability of precipitation is controlled by the interannual variability of the frontal activity. In order to identify the main features of the precipitation variability pattern an EOF analysis of the seasonal precipitation anomalies over southern South America was calculated. Figure 7 shows the leading mode of variability at the interannual timescales. In winter (Fig. 7a) the leading mode explains a 22 % of the total variance and it is characterized by centres of positive anomalies over SESA, the Atlantic Ocean and centre of Chile whereas negative anomalies are located to the southern part of the domain. In spring the first mode of precipitation variability explains 26 % of the total variance and shows negative anomalies over SESA, the Atlantic Ocean and centre and southern Chile whereas positive anomalies are located over the northeast and southern part of the domain. It can be seen that during both winter (Fig. 7a) and spring (Fig. 7b) the leading patterns of the interannual variability of precipitation are similar to those displayed in Fig. 6a, b, respectively. This may suggest that for the two seasons the leading mode of variability of precipitation over southern South America is controlled by the variability of the frontal activity at the interannual timescales. In order to quantify the contribution of the frontal activity variability to the variability of precipitation,

the correlation coefficient between PC1 of FI (using ERA Interim reanalysis) and PC1 of precipitation was calculated. For winter and spring the coefficient is 0.52 and 0.6, respectively (both coefficients being statistically significant with a confidence level of 95 %). This result suggests that 52 % (60 %) of the first mode of precipitation variability is associated with the first mode of variability of fronts in winter (spring). These results were also obtained using NCEP2 reanalysis (not shown), though with lower correlation coefficients.

4 Summary and conclusions

The variability of the frontal activity and its relationship with the circulation and precipitation variability at the interannual timescales is studied in this paper. The analysis is performed in austral winter and spring for the period 1979–2013, using two reanalysis datasets: the ERA Interim and the NCEP2. The analysis has three main objectives: (1) to identify the main modes of variability of fronts; (2) to explore the influence of the circulation variability on the frontal activity variability and (3) to identify the impact of the frontal activity variability on precipitation.

For winter the leading mode of interannual variability of fronts over the western SH depicts centres of positive and negative anomalies located especially over the southern part of the domain. In spring, the pattern is similar but is located further to the south (following the seasonal displacement of storm-tracks). These patterns were

detected from the two reanalysis datasets, reinforcing the idea that is robust. Positive (negative) anomalies of FI match negative (positive) anomalies of the 500 hPa geopotential height suggesting that cyclonic (anticyclonic) height anomalies favour (inhibit) the frontal activity, as expected.

Concerning the second objective, it was shown that both the SAM and ENSO-mode influence the leading mode of variability of FI for both winter and spring seasons. For the ERA-Interim dataset the correlation coefficients for winter between the first and the second PCs of the 500 hPa geopotential heights (SAM and ENSO-mode, respectively) against the PC1 of FI are 0.51 and 0.68, respectively. The correlations for spring are 0.34 and 0.67, respectively. Clearly, the ENSO phenomenon has more influence in the leading mode of fronts in both seasons, although the SAM is relevant also in wintertime.

The relationship between the variability of the frontal activity and precipitation was explored by means of a regression analysis between the leading mode of variability of FI and precipitation. For winter the regression showed a pattern of significant anomalies over SESA, centre of Chile and the mid-latitudes of the Pacific and Atlantic Oceans and anomalies of opposite sign in an area covering south of Chile and southeastern Pacific Ocean. In spring, the regression displayed precipitation anomalies over SESA and anomalies of opposite sign over southeast of Brazil and southern of the South American continent. Moreover, the areas where precipitation depicts strong interannual variability agree with areas where the precipitation anomalies associated with the variability of frontal activity are large, suggesting that the FI variability has a relevant role on the precipitation variability. In addition, the pattern of precipitation anomalies associated with the interannual variability of the FI agree with the leading mode of variability of precipitation over southern South America, reinforcing the idea that the interannual variability of FI exerts a dominant influence on the precipitation variability. Moreover, it was found that 52 (for winter) and 60 % (for spring) of the variability of precipitation corresponding to the first mode is associated with the leading mode of FI.

Summarizing, for both winter and spring, the leading mode of FI is conditioned by the SAM and ENSO variability modes of the large scale circulation and in turn the FI mode largely controls the pattern of precipitation variability.

Finally, the outcomes obtained in this study are complemented by the results of BS16. The two works analysed the role of the frontal activity variability as a link between atmospheric circulation variability and precipitation variability. This study focusing on the analysis at the interannual timescales and BS16 was devoted to the intraseasonal timescales.

References

Adler RF, Huffman GJ, Chang A, Ferraro R, Xie P, Janowiak J, Rudolf B, Schneider U, Curtis S, Bolvin D, Gruber A, Susskind J, Arkin P (2003) The version 2 global precipitation climatology project (GPCP) monthly precipitation analysis (1979-present). J Hydrometeorol 4:1147–1167. doi:10.1175/1525-7541(2003)004<1147:TVGPCP>2.0.CO;2

Bjerknes J, Solberg H (1922) Life cycle of cyclones and the polar front theory of atmospheric circulation. Geophys Publ 3:1–18

Blázquez J, Solman SA (2016) Intraseasonal variability of wintertime frontal activity and its relationship with precipitation anomalies in the vicinity of South America. Clim Dyn 46:2327–2336. doi:10.1007/s00382-015-2704-0

Browning KA, Roberts NM (1994) Structure of a frontal cyclone. Q J R Meteorol Soc 120:1535–1557. doi:10.1002/qj.49712052006

Catto JL, Jakob C, Berry G, Nicholls N (2012) Relating global precipitation to atmospheric fronts. Geophys Res Lett. doi:10.1029/2012GL051736

Dee DP et al (2011) The ERA-interim reanalysis: configuration and performance of the data assimilation system. Q J R Meteorol Soc 137:553–597. doi:10.1002/qj.828

Garreaud RD, Battisti DS (1999) Interannual (ENSO) and interdecadal (ENSO-like) variability in the Southern Hemisphere tropospheric circulation. J Clim 12:2113–2123

Grainger S, Frederiksen CS, Zheng X, Fereday D, Folland CK, Jin EK, Kinter JL, Knight JR, Schubert S, Syktus J (2011) Modes of variability of Southern Hemisphere atmospheric circulation estimated by AGCMs. Clim Dyn 36:473–490. doi:10.1007/s00382-009-0720-7

Grimm AM (2011) Interannual climate variability in South America: impacts on seasonal precipitation, extreme events, and possible effects of climate change. Stoch Environ Res Risk Assess 25:537–554. doi:10.1007/s00477-010-0420-1

Hannachi A, Jolliffe IT, Stephenson DB (2007) Empirical orthogonal functions and related techniques in atmospheric science: a review. Int J Climatol 27:1119–1152. doi:10.1002/joc.1499

Kanamitsu M, Ebisuzaki W, Woollen J, Yang S-K, Hnilo JJ, Fiorino M, Potter GL (2002) NCEP-DOE AMIP-II reanalysis (R-2). Bull Am Meteorol Soc 83:1631–1643. doi:10.1175/BAMS-83-11-1631

Kidson JW (1988) Interannual variations in the Southern Hemisphere circulation. J Clim 1:1177–1198. doi:10.1175/1520-0442(1988)001<1177:IVITSH>2.0.CO;2

Kidson JW (1999) Principal modes of Southern Hemisphere low-frequency variability obtained from NCEP–NCAR reanalyses. J Clim 12:2808–2830. doi:10.1175/1520-0442(1999)012<2808:PMOSHL>2.0.CO;2

Kiladis GN, Mo KC (1998) Interannual and intraseasonal variability in the Southern Hemisphere. In: Karoly DJ, Vincent DG (eds) Meteorology of the Southern Hemisphere, Chap 3. American Meteorological Society, pp 307–336. doi:10.1007/978-1-935704-10-2_11

Mo K (2000) Relationships between low-frequency variability in the Southern Hemisphere and sea surface temperature anomalies. J Clim 13:3599–3610. doi:10.1175/1520-0442(2000)013<3599:RBLFVI>2.0.CO;2

Mo KC, Nogés Paegle J (2001) The Pacific–South American modes and their downstream effects. Int J Climatol 21:1211–1229. doi:10.1002/joc.685

Rao VB, Do Carmo AMC, Franchito SH (2003) Interannual variations of storm tracks in the Southern Hemisphere and their connections with the Antartic Oscillation. Int J Climatol 23:1537–1545. doi:10.1002/joc.948

Rudeva I, Simmonds I (2015) Variability and trends of global atmospheric frontal activity and links with large-scale modes of variability. J Clim. doi:10.1175/JCLI-D-14-00458.1

Silvestri GE, Vera CS (2003) Antarctic Oscillation signal on precipitation anomalies over southeastern South America. Geophys Res Lett 30(21):2115. doi:10.1029/2003GL018277

Simmons A, Uppala S, Dee D, Kobayashi S (2007) ERA-interim: new ECMWF reanalysis products from 1989 onwards. ECMWF Newsl 110:25–35

Solman SA, Menéndez CG (2002) ENSO-related variability of the Southern Hemisphere winter storm track over the eastern Pacific-Atlantic sector. J Atmos Sci 59:2128–2141

Solman AS, Orlanski I (2010) Subpolar high anomaly preconditioning precipitation over South America. J Atmos Sci 67:1526–1542. doi:10.1175/2009JAS3309.1

Solman SA, Orlanski I (2014) Poleward shift and change of frontal activity in the Southern Hemisphere over the last 40 years. J Atmos Sci 71:539–552. doi:10.1175/JAS-D-13-0105.1

Thompson DWJ, Wallace JM (2000) Annular modes in the extratropical circulation. Part I: month-to-month variability. J Clim 13:1000–1016. doi:10.1175/1520-0442(2000)013<1000:AMITEC>2.0.CO;2

Trenberth KE, Stepaniak DP, Smith L (2005) Interannual variability of patterns of atmospheric mass distribution. J Clim 18:2812–2825. doi:10.1175/JCLI3333.1

Vera C (2003) Interannual and interdecadal variability of atmospheric synoptic scale activity in the Southern Hemisphere. J Geophys Res 108(C4):8077. doi:10.1029/2000JC000406